Compressible Problem

A grid of 35×35 cells is used with Neumann boundary conditions only. The domain consists of layers with two different permeability values (see Figure 1). The first layer has a permeability of $\sigma_1 = 30mD$, and the permeability of the second layer is $\sigma_2 = 3mD$. Therefore the permeability contrast between the layers is 10^{-1}.The initial pressure of the reservoir is set as 200 bars. Four wells are positioned in the corners of the domain with a bhp of 100 bars, and a well is placed in the center of the domain with a bhp of 600 bars. For the first set of problems, we use the updated solution of the first 10 time steps with the same configuration as the problem as deflation vectors. We solve the rest of the time steps with DICCG_{10} method with the 10 snapshots as deflation vectors and with 5 basis POD vectors as deflation vectors, DICCG_{POD}. For the second set of experiments, we use the same configuration as in the original problem but we vary the configuration of the wells. One corner well has the same pressure as the reservoir (200 bar), the other corner wells have a pressure of 100 bars and the central well has a pressure of 500 bars.

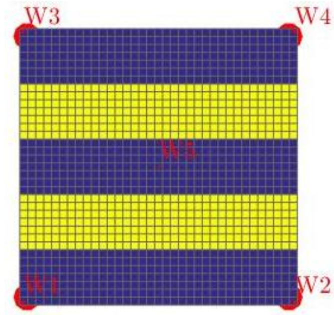

Figure 1: Heterogeneous permeability, 5 wells, compressible problem.

System configuration

Initial pressure 200 bar.

W1 = W2 = W3 = W4 = 100 bar.

W5 = 600 bars.

Boundary conditions :

$$\frac{\partial P(y=1)}{\partial n} = \frac{\partial P(y=ny)}{\partial n} = \frac{\partial P(x=1)}{\partial n} = \frac{\partial P(x=nx)}{\partial n} = 0.$$

Snapshots (second set of experiments)

$\mathbf{z}_1$: W2 = W3 = W4 = 100 bars, W1 = 200 bars, W5 = 500 bars.

$\mathbf{z}_2$: W1 = W3 = W4 = 100 bars, W2 = 200 bars, W5 = 500 bars.

$\mathbf{z}_3$: W1 = W2 = W4 = 100 bars, W3 = 200 bars, W5 = 500 bars.

$\mathbf{z}_4$: W1 = W2 = W3 = 100 bars, W4 = 200 bars, W5 = 500 bars.

The simulation was performed during 152 days with 52 time steps and a time step of 3 days. The tolerance of the NR method and the linear solvers is 10^{-5}.

Case 1

In Figure 14, the solution obtained with the ICCG method is presented, the solution is the same for all methods. The upper left figure represents the pressure field at the final time step. The upper right figure represents the pressure across the diagonal joining the (0,0) and (35,35) grid cells for all the timesteps. We observe the initial pressure (200 bars) in this diagonal and the evolution of the pressure field through time. In the lower figure we observe the surface volume rate for the five wells during the simulation.

1 NumSteps 13

The eigenvalues of the matrices are presented in Figure 15 for the original system matrix $\mathbf{J}$ for the first timestep, Figure 30 for the preconditioned system, Figure 32 the deflated system $DICCG_{10}$ and Figure 34 the deflated system combined with POD $DICCG_{POD}$ using the eigenvectors corresponding to the five largest eigenvalues. The eigenvalues of the snapshot correlation matrix $\mathbf{R} = \frac{1}{m}\mathbf{Z}\mathbf{Z}^T$ are presented in Figure 16.

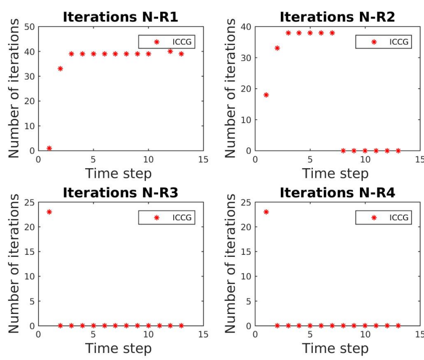

Figure 2: Number of iterations of the ICCG method for the first four NR iterations.

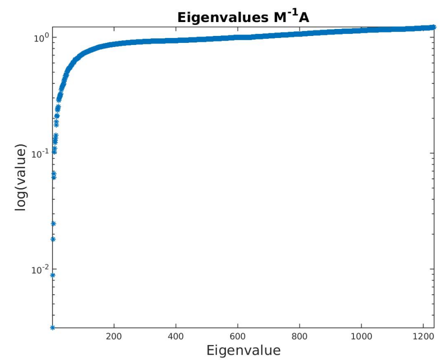

Figure 3: Eigenvalues of the preconditioned matrix, time step 1.

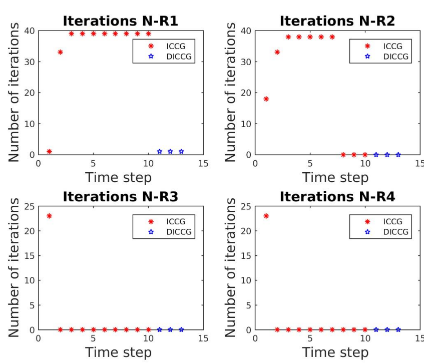

Figure 4: Number of iterations of the DICCG_{10} method for the first four NR iterations.

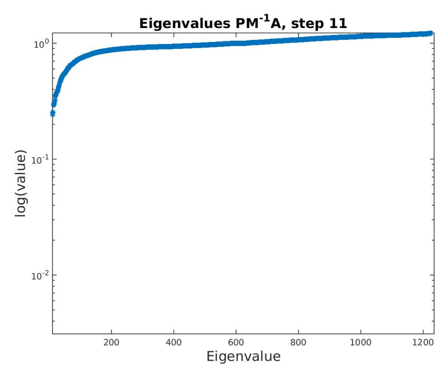

Figure 5: Eigenvalues of the deflated system DICCG_{10} with 10 deflation vectors.

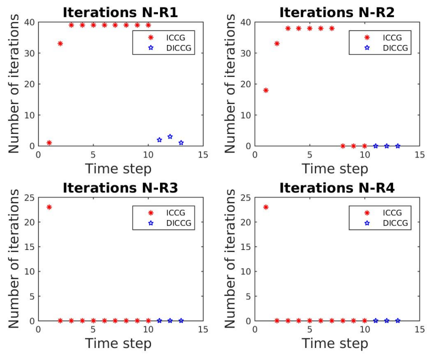

Figure 6: Number of iterations of the DICCG$_{POD}$ method for the first four NR iterations, eigenvectors [6-10].

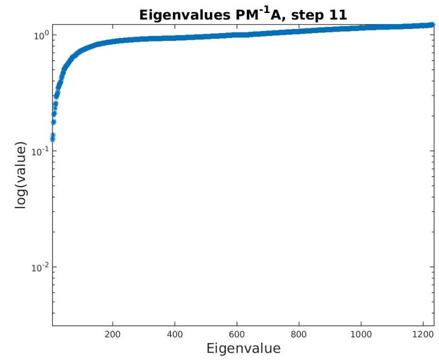

Figure 7: Eigenvalues of the deflated system DICCG$_{POD}$ with 10 deflation vectors, eigenvectors [6-10].

2 NumSteps 26

The eigenvalues of the matrices are presented in Figure 15 for the original system matrix $\mathbf{J}$ for the first timestep, Figure 30 for the preconditioned system, Figure 32 the deflated system $DICCG_{10}$ and Figure 34 the deflated system combined with POD $DICCG_{POD}$ using the eigenvectors corresponding to the five largest eigenvalues. The eigenvalues of the snapshot correlation matrix $\mathbf{R} = \frac{1}{m}\mathbf{Z}\mathbf{Z}^T$ are presented in Figure 16.

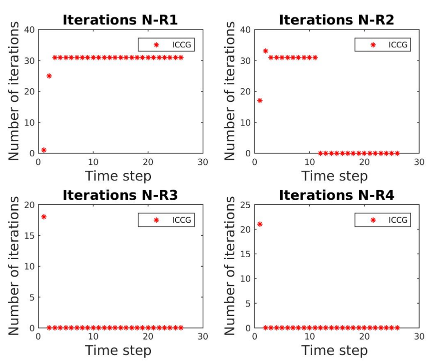

Figure 8: Number of iterations of the ICCG method for the first four NR iterations.

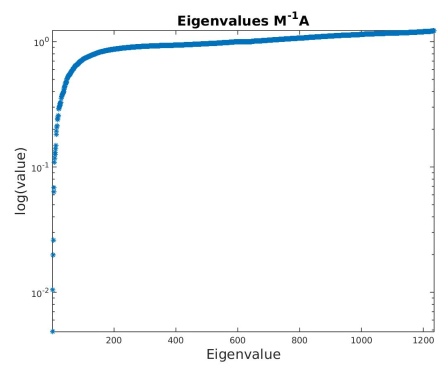

Figure 9: Eigenvalues of the preconditioned matrix, time step 1.

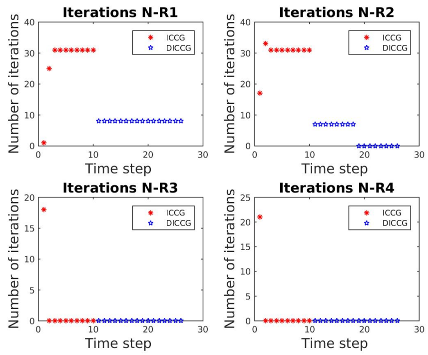

Figure 10: Number of iterations of the DICCG$_{10}$ method for the first four NR iterations.

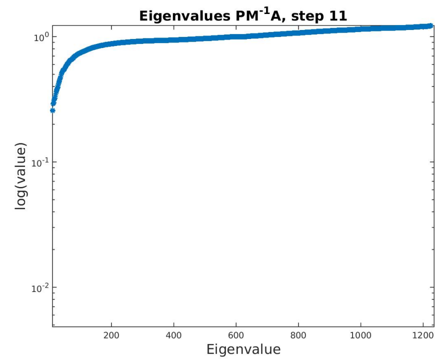

Figure 11: Eigenvalues of the deflated system DICCG$_{10}$ with 10 deflation vectors.

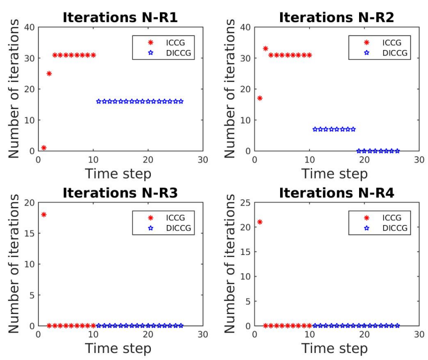

Figure 12: Number of iterations of the DICCG$_{POD}$ method for the first four NR iterations, eigenvectors [6-10].

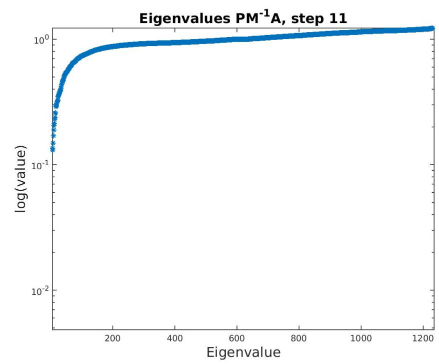

Figure 13: Eigenvalues of the deflated system DICCG$_{POD}$ with 10 deflation vectors, eigenvectors [6-10].

3 NumSteps 52

The number of iterations necessary to reach convergence with the linear solvers is presented for the first four NR iterations in Figure 29 for the ICCG method, Figure 31 for the deflated method DICCG$_{10}$ using 10 snapshots as deflation vectors and Figure 33, DICCG$_{POD}$, using the first 5 basis vectors of POD as deflation vectors. The eigenvalues of the matrices are presented in Figure 15 for the original system matrix **J** for the first timestep, Figure 30 for the preconditioned system, Figure 32 the deflated system $DICCG_{10}$ and Figure 34 the deflated system combined with POD $DICCG_{POD}$ using the eigenvectors corresponding to the five largest eigenvalues. The eigenvalues of the

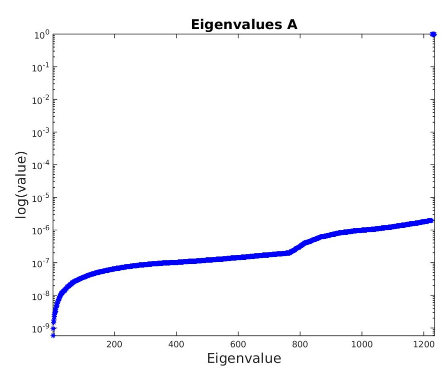

Figure 15: Eigenvalues of the original matrix **J**, time step 1.

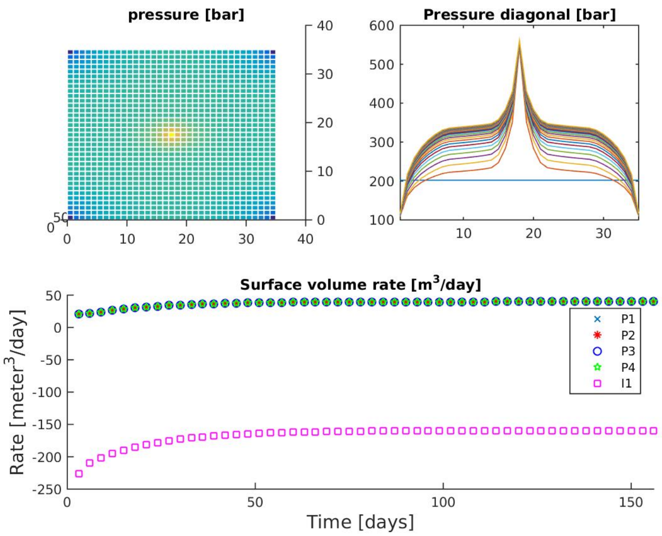

Figure 14: Solution of the compressible problem solved with the ICCG method.

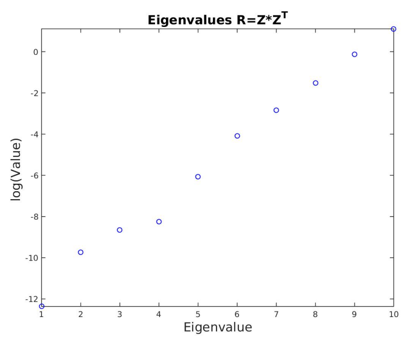

Figure 16: Eigenvalues of POD matrix, 10 deflation vectors.

snapshot correlation matrix $\mathbf{R} = \frac{1}{m}\mathbf{Z}\mathbf{Z}^T$ are presented in Figure 16.

We observe that the number of iterations for the first and second NR iterations is lower for the deflated methods compared with the ICCG method. However, we observe that the time step when convergence is achieved for the NR cycle is larger for these methods with respect to the ICCG method. We also observe that for the first NR iteration, the decrease is larger for the deflated method with 10 snapshots as deflation vectors.

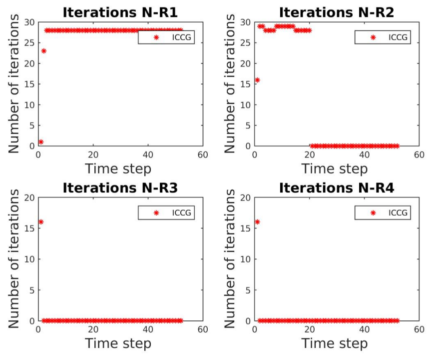

Figure 17: Number of iterations of the ICCG method for the first four NR iterations.

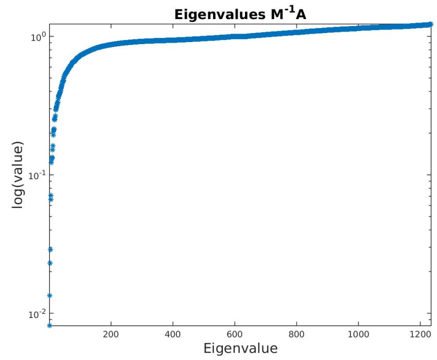

Figure 18: Eigenvalues of the preconditioned matrix, time step 1.

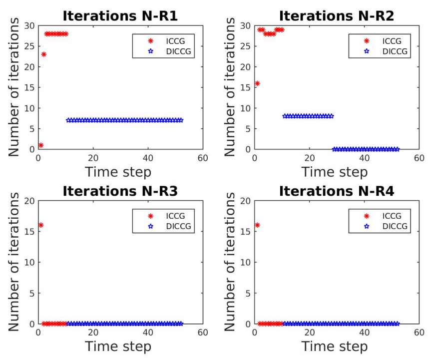

Figure 19: Number of iterations of the DICCG$_{10}$ method for the first four NR iterations.

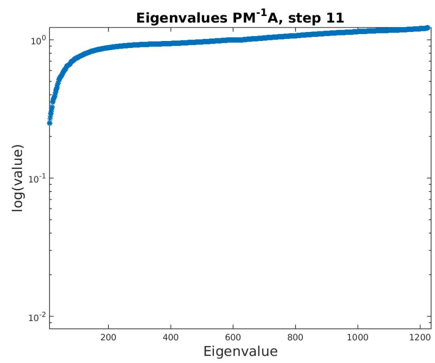

Figure 20: Eigenvalues of the deflated system DICCG$_{10}$ with 10 deflation vectors.

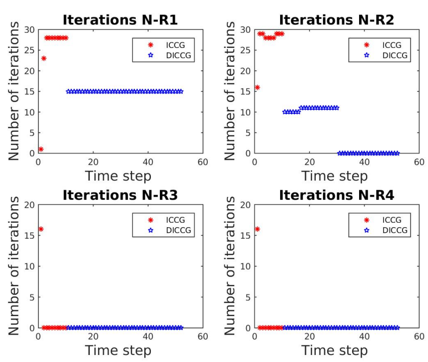

Figure 21: Number of iterations of the DICCG$_{POD}$ method for the first four NR iterations, eigenvectors [6-10].

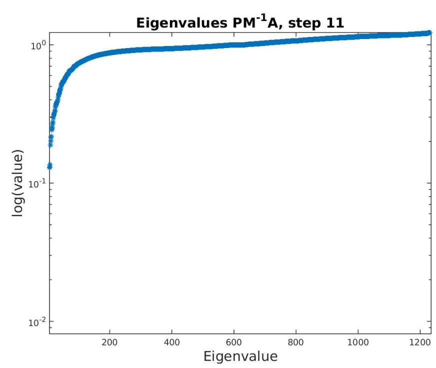

Figure 22: Eigenvalues of the deflated system DICCG$_{POD}$ with 10 deflation vectors, eigenvectors [6-10].

4 NumSteps 104

The eigenvalues of the matrices are presented in Figure 15 for the original system matrix **J** for the first timestep, Figure 30 for the preconditioned system, Figure 32 the deflated system $DICCG_{10}$ and Figure 34 the deflated system combined with POD $DICCG_{POD}$ using the eigenvectors corresponding to the five largest eigenvalues. The eigenvalues of the snapshot correlation matrix $\mathbf{R} = \frac{1}{m}\mathbf{Z}\mathbf{Z}^T$ are presented in Figure 16.

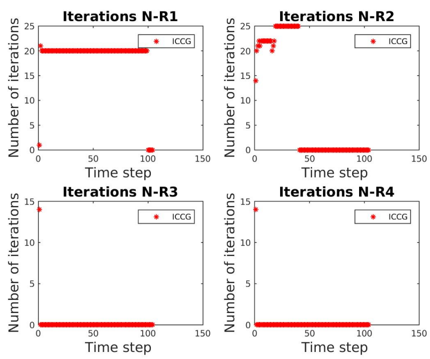

Figure 23: Number of iterations of the ICCG method for the first four NR iterations.

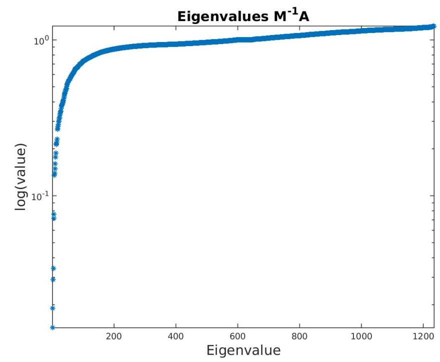

Figure 24: Eigenvalues of the preconditioned matrix, time step 1.

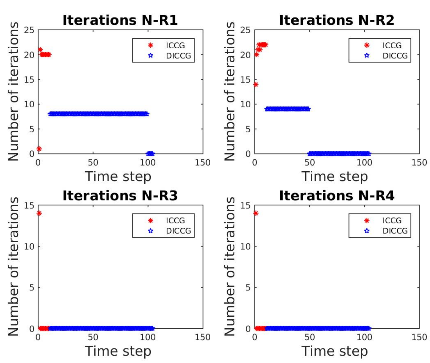

Figure 25: Number of iterations of the DICCG$_{10}$ method for the first four NR iterations.

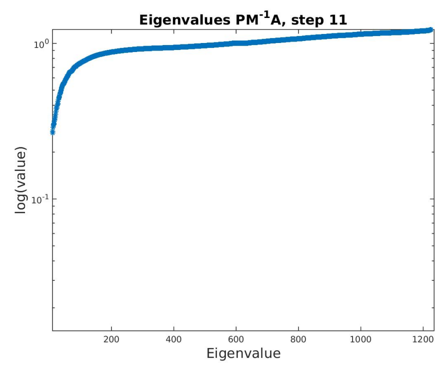

Figure 26: Eigenvalues of the deflated system DICCG$_{10}$ with 10 deflation vectors.

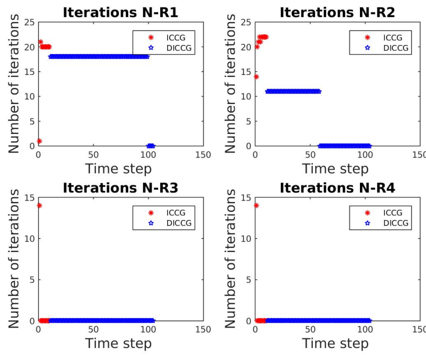

Figure 27: Number of iterations of the DICCG_{POD} method for the first four NR iterations, eigenvectors [6-10].

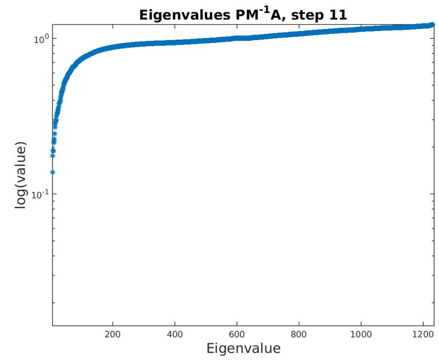

Figure 28: Eigenvalues of the deflated system DICCG_{POD} with 10 deflation vectors, eigenvectors [6-10].

5 NumSteps 156

The eigenvalues of the matrices are presented in Figure 15 for the original system matrix $\mathbf{J}$ for the first timestep, Figure 30 for the preconditioned system, Figure 32 the deflated system $DICCG_{10}$ and Figure 34 the deflated system combined with POD $DICCG_{POD}$ using the eigenvectors corresponding to the five largest eigenvalues. The eigenvalues of the snapshot correlation matrix $\mathbf{R} = \frac{1}{m}\mathbf{Z}\mathbf{Z}^T$ are presented in Figure 16.

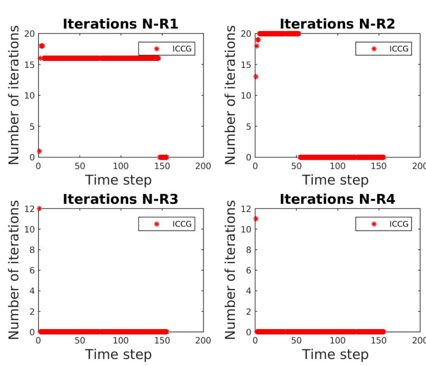

Figure 29: Number of iterations of the ICCG method for the first four NR iterations.

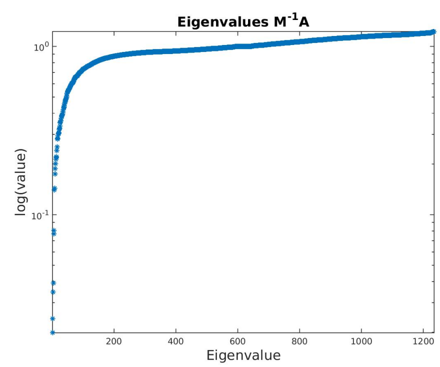

Figure 30: Eigenvalues of the preconditioned matrix, time step 1.

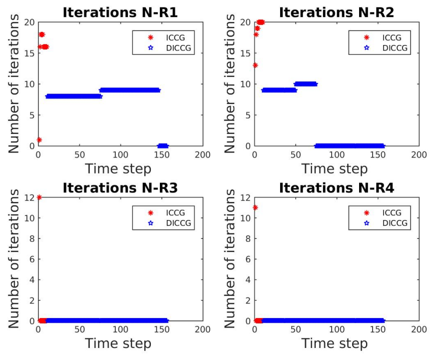

Figure 31: Number of iterations of the DICCG_{10} method for the first four NR iterations.

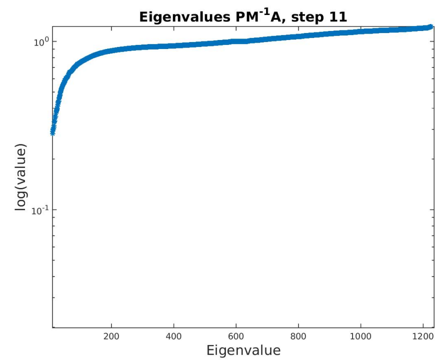

Figure 32: Eigenvalues of the deflated system DICCG_{10} with 10 deflation vectors.

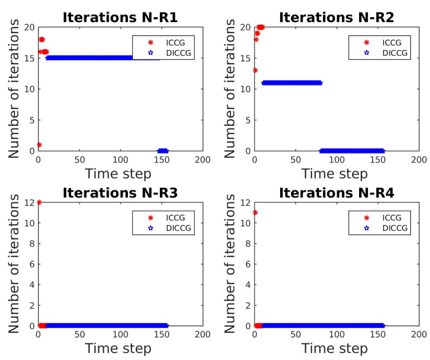

Figure 33: Number of iterations of the DICCG_{POD} method for the first four NR iterations, eigenvectors [6-10].

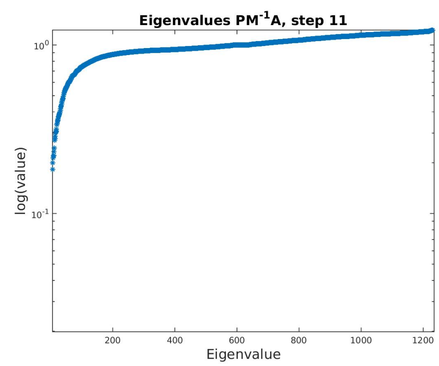

Figure 34: Eigenvalues of the deflated system DICCG_{POD} with 10 deflation vectors, eigenvectors [6-10].

Case 2

In the second case, we compute the first 4 time steps varying the bhp of the wells, as described above. Figure 35 presents the solution obtained with ICCG method is presented. The upper left figure represents the pressure field at the final time step. The upper right figure represents the pressure across the diagonal joining the (0,0) and (35,35) grid cells. We can observe the initial pressure (200 bars) in this diagonal and the evolution of the pressure field through the time. In the lower figure, we observe the surface volume rate for the five wells during the simulation.

The number of iterations necessary to achieve convergence with the linear solvers for this second problem is presented for the first four NR iterations in Figure 36 for the ICCG method, Figure 37 for the deflated method DICCG_{10} using 10 snapshots as deflation vectors and Figure 38 DICCG_{POD} using 5 basis vectors of POD as deflation vectors.

As in the previous case, we observe that the number of iterations for the first and second NR iterations is lower for the deflated methods compared with the ICCG method. However, we observe that the time step when convergence is achieved for the NR cycle is

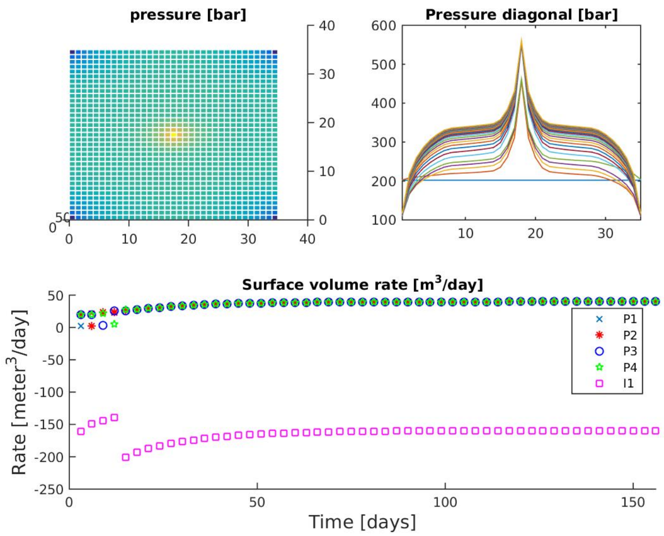

Figure 35: Solution of the compressible problem solved with the ICCG method, varying the bhp of the first 4 time steps.

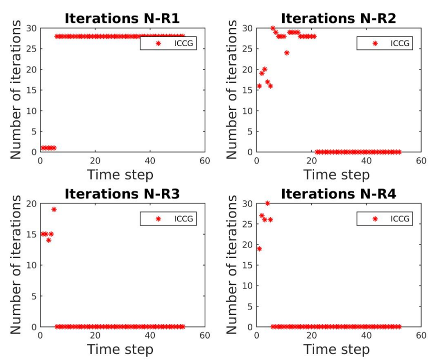

Figure 36: Number of iterations of the ICCG method for the first four NR iterations.

larger for these methods with respect to the ICCG method. We also observe that for the first NR iteration, the reduction is larger for the deflated method with 10 snapshots as deflation vectors.

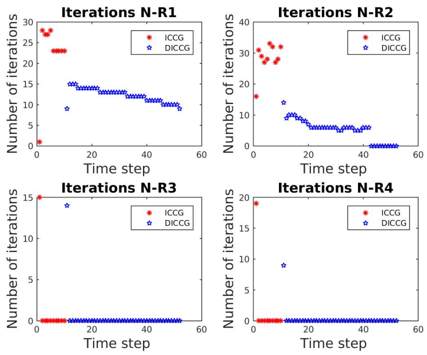

Figure 37: Number of iterations of the DICCG_{10} method for the first four NR iterations.

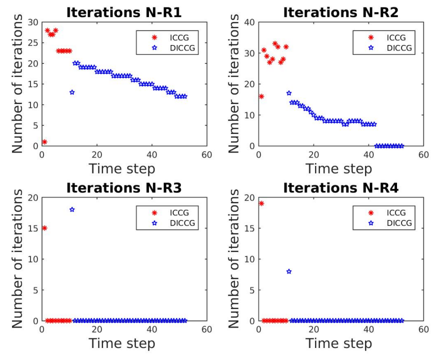

Figure 38: Number of iterations of the DICCG_{POD} method for the first four NR iterations.

References